ИНСТИТУТ ЯДЕРНОЙ ФИЗИКИ
СО АН СССР

V.L.Chernyak, I.R.Zhitnitsky

CALCULATION OF THE $\gamma\gamma \to \pi^0\pi^0$ CROSS SECTION AT HIGH ENERGIES

PREPRINT 82-44

Новосибирск

CALCULATION OF THE $\gamma\gamma - \rho^0\rho^0$ CROSS SECTION AT HIGH ENERGIES

V.L.CHERNYAK, I.R.ZHITNITSKY

Institute of Nuclear Physics

630090, Novosibirsk, USSR

ABSTRACT

The processes with the cross sections not decreasing with energy become important at high energies. The simplest processes of this kind are $\gamma\gamma - V_i^0 V_j^0$ where $V^0 = \rho^0, \omega, \varphi, \ldots$ We calculate their cross sections in the high energy small angle region $S \gg |t| \gg M^2$. The cross section $\gamma\gamma - \rho^0\rho^0$ exceeds at high energies ($S \gtrsim 10\ GeV^2$) those of $\gamma\gamma - \pi\pi, \rho^+\rho^-$ considerably. At $S \simeq 10^4\ GeV^2$ (this is the characteristic energy for the VLEPP and SLC colliders) and $|t| \simeq 2 GeV^2$ the ratio $\frac{d\sigma}{dt}(\gamma\gamma - \rho^0\rho^0) \Big/ \frac{d\sigma}{dt}(\gamma\gamma - \mu^+\mu^-) \simeq 70$.

I. Introduction.

The role of investigations of the process "$\gamma\gamma \to$ hadrons" is at present increasing, see /1/. Interesting experimental information was obtained in the last years at existing accelerators at DESY and SLAC. New prospects will be opened by linear electron-positron colliders such as the VLEPP project at Novosibirsk ($\sqrt{S} \simeq 100$-$300\ GeV$) and SLC at Stanford ($\sqrt{S} \simeq 50$-$70\ GeV$) /2,3/. It is shown in /4/ that e^+e^- beams can be converted into the $\gamma\gamma$ beams for these colliders without considerable losses in the energy and the luminosity.

It is clear that the processes with the cross sections not decreasing with energy are of importance at high energies. These are the processes with the vacuum quantum numbers in the t-channel. In this paper the simplest exclusive process of such a kind, $\gamma\gamma \to \rho^0\rho^0$ scattering, is considered, fig. 1. The calculation of the cross section is performed in the region $S \gg |t| \gg M^2$. The condition $|t| \gg M^2$ ensures large virtualities in the t-channel and so allows one to use the QCD perturbation theory. We confine ourselves here by the simplest non-trivial diagrams like those in fig. 2. This approximation can be considered as the "bare Pomeranchuk singularity" exchange. The calculation of the $\gamma\gamma \to \rho^0\rho^0$ cross section is described in sect. II. The discussion of the results and comparison with the $\gamma\gamma \to \pi^+\pi^-, \pi^0\pi^0, \rho^+\rho^-$ cross sections are presented in sect. III.

II. The $\gamma\gamma \to \rho^0\rho^0$ cross section at high energies.

Below the contribution of the diagrams like those in fig.2 into the $\gamma\gamma \to \rho^0\rho^0$ cross section is calculated. The general method for finding the asymptotic behaviour of the exclusive proccesses in QCD is developed in [5-11]. Therefore we give below the results only. Let us point only the following: i) the perturbation theory propagators can be used at $|t| \gg \mu^2$ because the propagator virtualities in fig.2 are $\gtrsim O(t)$; ii) only the ρ_L -mesons with the zero helicity are produced; iii) each of the diagrams like those in fig.2 give a contribution $\sim (s/t^2) \cdot \ln\frac{s}{t}\ln\frac{t}{\mu^2}$ but all the logarithms cancel in the sum of the diagrams.

The amplitude of the $\gamma\gamma \to \rho^0\rho^0$ process is pure imaginary at $s \gg |t| \gg \mu^2$ and has the form:

$$M = i\left(4\pi\alpha\right)\left(4\pi\alpha_s\right)^2 \frac{s}{t}\frac{f_\rho^2}{t}\frac{4}{9\pi}\int_{-1}^{1} d\xi_1 \varphi_\rho(\xi_1)\int_{-1}^{1} d\xi_2 \varphi_\rho(\xi_2) M_0(\xi_1,\xi_2),$$

$$M_0(\xi_1,\xi_2) = (e^{\lambda_1}\cdot n)(e^{\lambda_2}\cdot n)\frac{\xi_1\cdot\xi_2}{(1-\xi_1^2)(1-\xi_2^2)}\left[2\frac{1-\xi_2^2}{\xi_1-\xi_2}+\xi_1\right]\ln\frac{1+\xi_2}{1-\xi_2} + \quad (1)$$

$$+ (e^{\lambda_1}\cdot e^{\lambda_2})\frac{\xi_1\cdot\xi_2}{(1-\xi_1^2)(1-\xi_2^2)}\left[\ln|\xi_1-\xi_2| + \frac{1-\xi_2^2}{\xi_1-\xi_2}\ln\frac{1+\xi_2}{1-\xi_2}\right],$$

$$n_\mu = p_\mu/\sqrt{|t|}.$$

Here: $\alpha = 1/137$, e^{λ_1}, e^{λ_2} are the photon polarization vectors, $f_\rho \simeq 200$ MeV, $\varphi_\rho(\xi)$ is the ρ_L -meson wave function determined by the matrix element

$$\langle 0|\bar u(+z)\gamma_\mu u(-z) - \bar d(+z)\gamma_\mu d(-z)/\sqrt{2}\,|\rho_L^0(p)\rangle_{\mu_0} = p_\mu f_\rho \varphi_\rho(zp) + \ldots \quad (2)$$

$$\varphi_\rho(zp) = \int_{-1}^{1} d\xi\, \varphi_\rho(\xi) e^{i\xi(zp)}, \quad \varphi_\rho(zp=0) = 1, \quad |\vec p| \to \infty.$$

The function $\varphi_\rho(\xi)$ determines the distribution of the ρ_L -meson longitudinal momentum between the quarks: $p = p_1 + p_2$, $p_1 = xp$, $p_2 = (1-x)p$, $\xi = 2x-1$. We use for the numerical calculation the wave function $\varphi_\rho(\xi)$ found in [12] using the QCD sum rules:

$$\varphi_\rho(\xi, \mu_0 \sim 0.5\,\text{GeV}) \simeq \frac{15}{4}\left(1-\xi^2\right)\left(0.3\xi^2 + 0.14\right) \quad (3)$$

(μ_0 is the normalization point of the wave function; the μ_0 -dependence of the wave function is determined by the renormalization group and actually is weak).

Using (1),(3) we have for the helicity amplitudes ($\pm$ indicate the photon helicities):

$$M^{++} = M^{--} \simeq i\frac{s}{t}\frac{f_\rho^2}{t}\left(4\pi\alpha\right)\left(4\pi\alpha_s\right)^2\frac{1}{\pi}1.1, \quad (4)$$

$$M^{+-} = M^{-+} \simeq i\frac{s}{t}\frac{f_\rho^2}{t}\left(4\pi\alpha\right)\left(4\pi\alpha_s\right)^2\frac{1}{\pi}0.8.$$

The $\gamma\gamma \to \rho^0\rho^0$ differential cross section is

$$\frac{d\sigma_\rho}{dt} = \frac{1}{16\pi s^2}\frac{1}{4}\sum_{\lambda_1\lambda_2}|M^{\lambda_1\lambda_2}|^2. \quad (5)$$

The ratio $d\sigma(\gamma\gamma\to\rho^0\rho^0)/d\sigma(\gamma\gamma\to\mu^+\mu^-)$ in the region $s \gg |t| \gg \mu^2$ is therefore:

$$d\sigma(\rho_L^0\rho_L^0)/d\sigma(\mu^+\mu^-) \simeq 240\pi^2\alpha_s^4\frac{f_\rho^4}{t^2}\frac{s}{|t|}. \quad (6)$$

At $|t|\simeq 2\,GeV^2$ and $f_\rho \simeq 0.2\,GeV$, $\alpha_s(t/4)\simeq 0.35$

$$\frac{d\sigma(\rho_L^0\rho_L^0)}{d\sigma(\mu^+\mu^-)} \simeq \begin{cases} 0.15 & \text{at } s\simeq 20\,GeV^2 \\ 70 & \text{at } s\simeq 10^4\,GeV^2 \end{cases} \qquad (7)$$

The production cross section looks as follows:

$$\tilde\sigma(\rho_L^0\rho_L^0) = \int_{t_{min}}^{s/2} dt\left(\frac{d\sigma}{dt}\right) \simeq 480\pi^3\alpha^2\alpha_s^4 f_\rho^4 \int_{t_{min}}^{s/2}\frac{dt}{t^4} \simeq$$

$$\simeq \frac{2.5\ nbn}{[t_{min}(GeV)]^3} \simeq 0.3\ nbn \quad \text{at } |t_{min}|\simeq 2GeV^2. \qquad (8)$$

The contributions of the fig.2 diagrams to the $\gamma\gamma-\omega\omega$ and $\gamma\gamma-\varphi\varphi$ cross sections are evidently given by the same formula (1) with the replacement: $f_\rho\psi_\rho(z)\to\frac{1}{3}f_\rho\psi_\rho(z)$ for the ω -meson and $f_\rho\psi_\rho(z)\to\frac{\sqrt{2}}{3}f_\varphi\psi_\varphi(z)$ for the φ -meson. The φ -meson wave function has been found in /12/ and has the form:

$$f_\varphi = 1.15 f_\rho \simeq 230\,MeV, \qquad \psi_\varphi(z) = \frac{3}{4}(1-z^2). \qquad (9)$$

Using these wave functions one has at $s\gg|t|\gg\mu^2$:

$$(\rho_L^0\rho_L^0)_{2gl} : (\omega_L\omega_L)_{2gl} : (\varphi_L\varphi_L)_{2gl} : (\rho_L\omega_L)_{2gl} \simeq 1 : \frac{1}{80} : \frac{1}{80} : \frac{1}{18}. \qquad (10)$$

The most characteristic feature of the production mechanism shown at fig.2 is the existence of the $\gamma\gamma\to\rho^0\varphi$ cross section. Using the wave function (9) one obtains at $s\gg|t|\gg\mu^2$

$$\frac{d\sigma(\gamma\gamma-\rho_L^0\varphi_L)}{dt} \simeq \frac{1}{20}\ \frac{d\sigma(\gamma\gamma-\rho_L^0\rho_L^0)}{dt} \qquad (11)$$

The production cross section is

$$\tilde\sigma(\rho^0\varphi) = \int_{t_{min}}^{s} dt\left(\frac{d\sigma(\rho\varphi)}{dt}\right) \simeq 3\cdot 10^{-2}\ nbn \quad \text{at } |t_{min}|\simeq 2GeV^2. \qquad (12)$$

Let us compare the cross section (8) with the total light meson production cross section at high energies (see fig. 5, /13,14/):

$$\frac{d\sigma}{dt} \simeq \frac{8}{9}\frac{\alpha_s^2}{\alpha^2}\left(\frac{16}{9\pi}\alpha^4\frac{1}{t^2}\ln^2\frac{t}{\mu^2}\right), \qquad (13)$$

where μ is the infrared cut off ($\mu^2\simeq\langle p_\perp^2\rangle\simeq(300\,MeV)^2$).
At $|t_{min}|\simeq 2GeV^2$, $\alpha_s\simeq 0.3$

$$\tilde\sigma_{tot}\simeq 5\ nbn, \qquad \tilde\sigma(\rho_L^0\rho_L^0)/\tilde\sigma_{tot} \sim 5-10\% \qquad (14)$$

III. Discussion.

1. The cross sections calculated above can be considered as the Born approximation. The loop corrections due to the diagrams like those in fig.3 become important at high energies, $s\gg|t|$. Each loop in fig.3 gives the factor

$$\sim\frac{\alpha_s(t)}{\pi}\ln s/|t|.$$

At $|t|\simeq 2GeV^2$ this factor is $\sim O(1)$ in the VLEPP or SLC region $s\simeq 10^4\,GeV^2$ and so the leading logarithm corrections should be taken into account in this region (we expect that at $s\simeq 10^4 - 10^2\,GeV^2$ the logarithmic corrections can be neglected). The result of summation of the leading logarithm contributions in the non-abelian gauge theories /15/ shows that these contributions increase the cross section. We expect therefore that the above calculated cross sections $\rho^0\rho^0$, $\rho^0\varphi$ give the limits from below and the real cross sections are larger.

2. It is of interest to compare the $\gamma\gamma\to\rho^0\rho^0$ cross section due to the fig.2 contribution with that of $\gamma\gamma\to\pi^{\pm0}\pi^{\mp0}$, $\rho^{\pm0}\rho^{\mp0}$

cross sections due to fig.4 contributions. These cross sections have been calculated in /16/ in terms of the meson wave functions. The wave functions used in /16/ in order to obtain the numerical predictions are however unrealistic, from our point of view. We use in the numerical calculations the π- and $\rho_{\perp,\parallel}$-meson wave functions obtained in /12,17/ using the QCD sum rules.

The π-meson wave function is determined by the matrix element $\langle 0|\bar{d}(z)\gamma_\mu\gamma_5 u(-z)|\pi(p)\rangle = ip_\mu f_\pi \cdot \int_{-1}^{1} d\xi\, \varphi_\pi(\xi) \exp\{i\xi(zp)\} + \ldots$ and has the form:

$$f_\pi \simeq 133\,\text{MeV}, \quad \varphi_\pi(\xi, M_0) \simeq \frac{15}{4}\left(1-\xi^2\right)\xi^2, \quad M_0 \sim 0.5\,\text{GeV}. \qquad (15)$$

The wave function of the $\rho_\parallel$-meson with zero helicity is given by (2),(3) and that of the $\rho_\perp$-meson with the helicity $|\lambda| = 1$ is determined by the matrix element ($e_\mu^\perp$ is the $\rho_\perp$-meson polarization vector)

$$\langle 0|\bar{d}(z) i\tfrac{1}{2}[\gamma_\mu,\gamma_\nu] u(-z)|\rho_\perp(p)\rangle = \left(e_\mu^\perp p_\nu - e_\nu^\perp p_\mu\right) f_T \int_{-1}^{1} d\xi\, e^{i\xi(zp)}\, \varphi_T(\xi),$$

and has the form:

$$f_T(M_0) \simeq 200\,\text{MeV}, \quad \varphi_T(\xi, M_0) \simeq \frac{15}{16}\left(1-\xi^2\right)^2, \quad M_0^2 \sim 0.5\,\text{GeV}^2. \qquad (16)$$

The behaviour of the cross sections is shown in figs. 6,7. Let us point the following:

a) the numerical values of all the cross sections (except for $\gamma\gamma \to \pi^+\pi^-$) differ essentially from those given in paper /16/;

b) the two-gluon exchange contribution, fig.2, into the $\gamma\gamma \to \rho_L^0\rho_L^0$ cross section (i.e. $\left(\rho_L^0\rho_L^0\right)_{2g}$, see fig.6) is at $\theta \simeq 90^\circ$ of the same order as the two-quark exchange contributions into the $\gamma\gamma \to \pi^+\pi^-, \rho_L^+\rho_L^-$ cross sections, fig.4. At smaller angles, however, the $\left(\rho_L^0\rho_L^0\right)_{2g}$ cross section is much larger than any other "$\gamma\gamma \to$ two mesons" cross section (see fig.6). Even the $\gamma\gamma \to \rho\varphi$ cross section is larger at small angles than $\gamma\gamma \to \rho^+\rho^-, \pi^+\pi^-$ (see fig.6).

We are grateful to V.G.Serbo for the useful discussion.

REFERENCES

/1/ 4-th Intern. Colloq. on Photon-photon Interactions, Paris, April, 1981

/2/ V.E.Balakin, G.I.Budker, A.N.Skrinsky, Preprint INP-78-101, Novosibirsk, 1978
V.E.Balakin, A.N.Skrinsky, "VLEPP Project (Status report)", Preprint INP-81-129, Novosibirsk, 1981

/3/ SLAC Report 229, 1980
B.Richter et.al., Preprint SLAC-PUB-2549, 1980
P.Panofsky, Report at Intern. Symp. on Lepton and Photon Interactions at High Energies, Bonn, 1981

/4/ I.F.Ginzburg, G.L.Kotkin, V.G.Serbo, V.I.Telnov, Pis'ma v Zh. Eksp. Teor. Fiz., 9 (1981) 514

/5/ V.L.Chernyak, A.R.Zhitnitsky, JETP Lett., 25 (1977) 510
V.L.Chernyak, A.R.Zhitnitsky, V.G.Serbo, JETP Lett., 26(1977) 594

V.L.Chernyak,A.R.Zhitnitsky, Yad.Fiz. 31 (1980) 1053
V.L.Chernyak,V.G.Serbo,A.R.Zhitnitsky, Yad.Fiz.31(1980)1069
V.L.Chernyak, Proc. XV-th Winter LINP School, vol. I, pp.65-155, Leningrad, 1980

/6/ D.R.Jackson, Ph. D. Thesis, Caltech, Pasadena, 1977
G.R.Farrar,D.R.Jackson, Phys Rev.Lett. 43 (1979) 246

/7/ A I Vainshtein,V I Zakharov, Phys.Lett. 72B (1978) 368

/8/ A.V.Efremov,A.V.Radyushkin, Phys.Lett 94B (1980) 245, Teor i Mat.Fiz 42 (1980) 147

/9/ G Parisi, Phys. Lett 84B (1979) 225

/10/ G.P Lepage,S.J Brodsky, Phys Lett 87B (1979) 359, Phys.Rev.Lett 43 (1979) 545, 43 (1979) 1625(E), Phys Rev. D22 (1980) 2157

/11/ A.Duncan, A.H Mueller, Phys.Rev D21 (1980) 1636, Phys. Lett. 90B (1980) 159, Phys.Lett 93B (1980) 119

/12/ V L Chernyak,A R Zhitnitsky,I R Zhitnitsky, Preprint INP-82-26, Novosibirsk, 1982

/13/ H Cheng,T.T Wu, Phys Rev D1 (1970) 3414

/14/ L N Lipatov,G V Frolov, Yad Fiz 13 (1971) 333

/15/ E A Kuraev,L N Lipatov,V S Fadin, Zh. Eksp Teor Fiz 71 (1976) 840, 72 (1977) 377

/16/ S.J.Brodsky,G.P.Lepage, Phys.Rev. D24 (1981) 1808

/17/ V.L.Chernyak,A.R.Zhitnitsky, Preprint INP-81-74, Novosibirsk, 1981

Figure captions

Fig.6. Predictions for the $\gamma\gamma \to \pi^+\pi^-$, $\rho_L^+\rho_L^-$, $\rho_L^0\rho_L^0$ and $\gamma\gamma \to \rho^0\varphi$ cross sections (ρ_L denotes the ρ -meson with the helicity $\lambda = 0$). The wave function of the ρ_L -meson is given by (2),(3). The contributions to the cross section $\gamma\gamma \to \rho_L^0\rho_L^0$ due to fig.2 and fig.4 are denoted by $(\rho_L^0\rho_L^0)_{2g}$ and $(\rho_L^0\rho_L^0)_{2q}$ respectively (α_s was taken $\alpha_s \approx 0.35$).

Fig.7. Predictions for the $\gamma\gamma \to \pi^0\pi^0$, $\rho_\perp^+\rho_\perp^-$ and $\gamma\gamma \to \rho_\perp^0\rho_\perp^0$ cross sections ($\rho_\perp$ denotes the ρ -meson with the helicity $|\lambda| = 1$). The wave functions of the π - and $\rho_\perp$ -mesons are given by the formulae (15),(16) respectively (α_s was taken $\alpha_s \approx 0.35$).

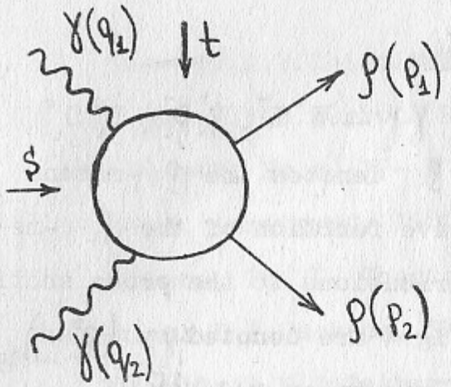

Fig. 1

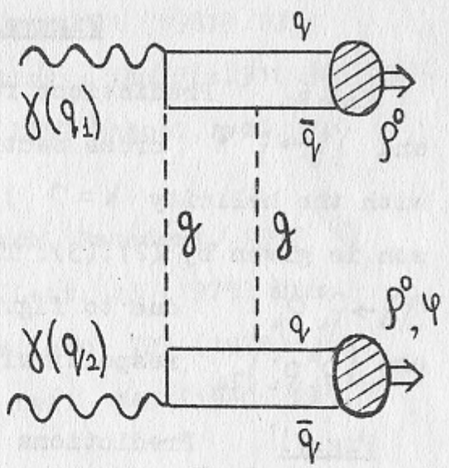

Fig. 2

Fig. 3

Fig. 4

Fig. 5

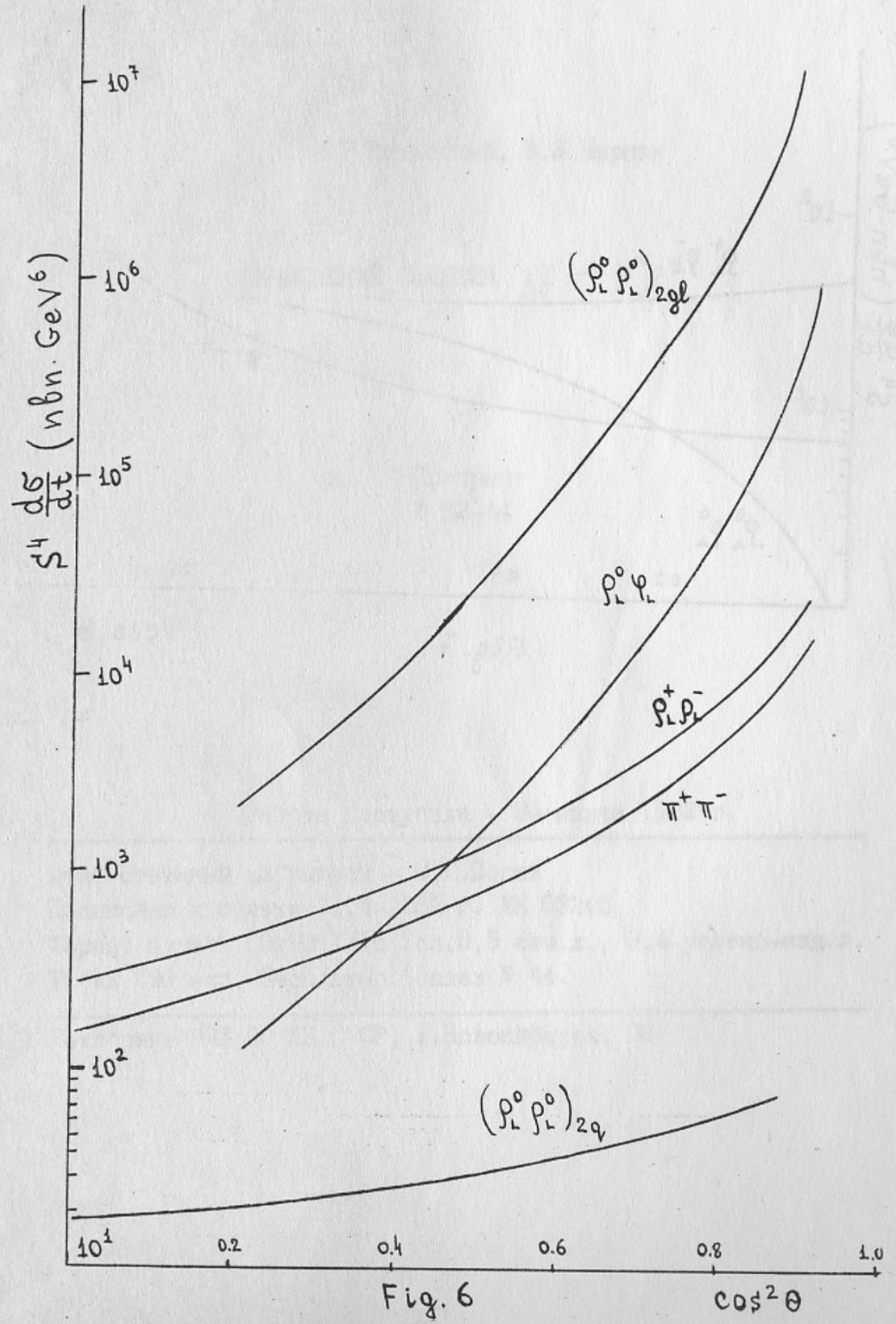

Fig. 6

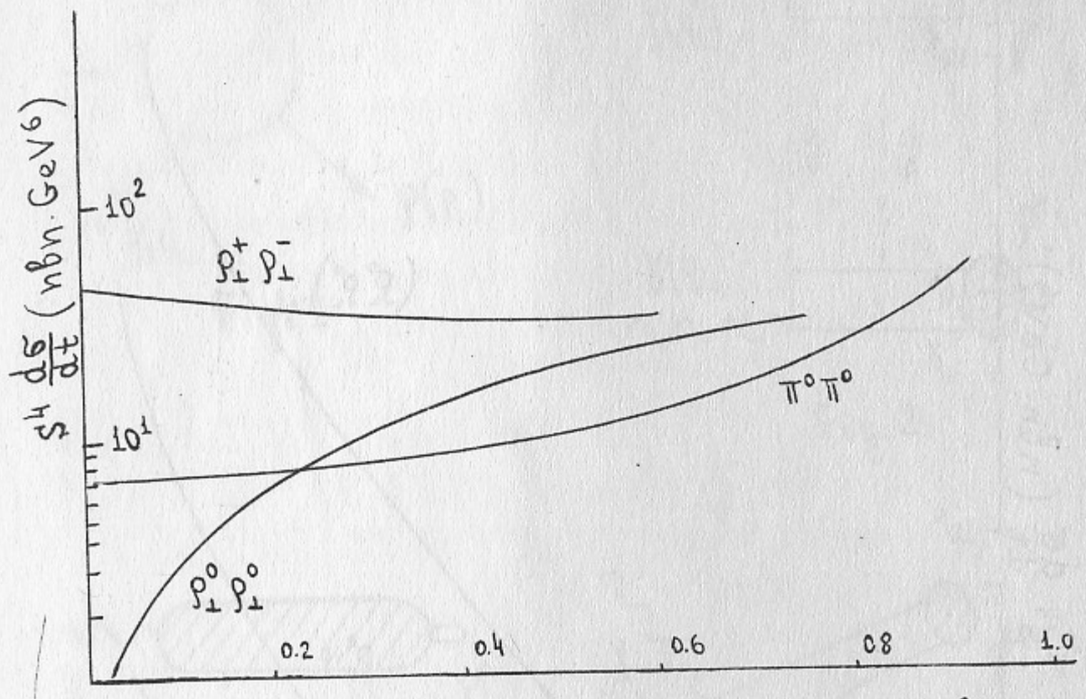

Fig.7

И.Р.Житницкий, В.Л.Черняк

ВЫЧИСЛЕНИЕ СЕЧЕНИЯ $\gamma\gamma \to \rho^0\rho^0$

Препринт
№ 82-44

Работа поступила - 30 марта 1982 г.

Ответственный за выпуск - С.Г.Попов
Подписано к печати 21.4-1982 г. МН 03245
Формат бумаги 60x90 1/16 Усл.0,5 печ.л., 0,4 учетно-изд.л.
Тираж 290 экз. Бесплатно. Заказ № 44.

Ротапринт ИЯФ СО АН СССР, г.Новосибирск, 90